HHS Public Access

Author manuscript

Neuroimage. Author manuscript; available in PMC 2024 November 02.

Published in final edited form as:

Neuroimage. 2024 November 01; 301: 120878. doi:10.1016/j.neuroimage.2024.120878.

Oscillatory activity in bilateral prefrontal cortices is altered by distractor strength during working memory processing

Megan C. Hall[a,1], **Maggie P. Rempe**[a,b,1], **Ryan J. Glesinger**[a], **Lucy K. Horne**[a], **Hannah J. Okelberry**[a], **Jason A. John**[a], **Christine M. Embury**[a], **Elizabeth Heinrichs-Graham**[a,c], **Tony W. Wilson**[a,c,*]

[a]Institute for Human Neuroscience, Boys Town National Research Hospital, 14090 Mother Teresa Lane, Boys Town, NE, 68010, USA

[b]College of Medicine, University of Nebraska Medical Center (UNMC), 42nd and Emile, Omaha, NE, 68198, USA

[c]Department of Pharmacology & Neuroscience, Creighton University, 2500 California Plaza, Omaha, NE, 68178, USA

Abstract

Working memory (WM) enables the temporary storage of limited information and is a central component of higher order cognitive function. Irrelevant and/or distracting information can have a negative impact on WM processing and suppressing such incoming stimuli is critical to maintaining adequate performance. However, the neural mechanisms and dynamics underlying such distractor inhibition remain poorly understood. In the current study, we enrolled 46 healthy adults (M_{age}: 27.92, N_{female}: 28) who completed a Sternberg type WM task with high- and low-distractor conditions during magnetoencephalography (MEG). MEG data were transformed into the time-frequency domain and significant task-related oscillatory responses were imaged to identify the underlying anatomical areas. Whole-brain paired *t*-tests, with cluster-based permutation testing for multiple comparisons correction, were performed to assess differences

*Corresponding author at: Institute for Human Neuroscience, Boys Town National Research Hospital, USA. tony.wilson@boystown.org (T.W. Wilson).

[1]Contributed equally.

Data and code availability

All data are publicly available via the Collaborative Informatics and Neuroimaging Suite (COINS; https://coins.trendscenter.org/) upon request.

CRediT authorship contribution statement

Megan C. Hall: Writing – original draft, Visualization, Methodology, Investigation, Formal analysis. **Maggie P. Rempe:** Writing – review & editing, Supervision, Project administration, Methodology, Investigation, Formal analysis, Conceptualization. **Ryan J. Glesinger:** Project administration, Data curation. **Lucy K. Horne:** Data curation. **Hannah J. Okelberry:** Project administration, Data curation. **Jason A. John:** Project administration, Data curation. **Christine M. Embury:** Writing – review & editing, Software, Conceptualization. **Elizabeth Heinrichs-Graham:** Supervision, Project administration. **Tony W. Wilson:** Writing – review & editing, Supervision, Project administration.

Declaration of competing interest

The authors declare that they have no known competing financial interests or personal relationships that could have appeared to influence the work reported in this paper.

Supplementary materials

Supplementary material associated with this article can be found, in the online version, at doi:10.1016/j.neuroimage.2024.120878.

between the low- and high-distractor conditions for each oscillatory response. Across conditions, we found strong alpha and beta oscillations (i.e., decreases relative to baseline) and increases in theta power throughout the encoding and maintenance periods. Whole-brain contrasts revealed significantly stronger alpha and beta oscillations in bilateral prefrontal regions during maintenance in high- compared to low-distractor trials, with the stronger beta oscillations being centered on the left dorsolateral prefrontal cortex and right inferior frontal gyrus, while those for alpha being within the right anterior prefrontal cortices and the right middle frontal gyrus. These findings suggest that alpha and beta oscillations in the bilateral prefrontal cortices play a major role in the inhibition of distracting information during WM maintenance. Our results also contribute to prior research on cognitive control and functional inhibition, in which prefrontal regions have been widely implicated.

Keywords

Magnetoencephalography (MEG); Cognitive control; Ventral attention network (VAN); Functional inhibition; Inhibitory control

1. Introduction

Working memory (WM) is necessary for remembering relevant information and is a central component of higher-level cognition. WM generally refers to the temporary storage of limited information that can be consolidated into long-term memory or forgotten after a brief period (Baddeley, 1983) and is served by multiple neural subsystems that are involved in other cognitive processes. Encoding and maintenance are two distinguishable stages of WM processing, with encoding referring to the processes of transforming sensory input into representations that are entered into some form of temporary memory buffer, while maintenance refers to the rehearsal of these representations occurring alongside related processes that are necessary for memory retention until the retrieval phase (Baddeley, 1992; D'Esposito and Postle, 2015; Woodman and Vogel, 2005). The amount of information that can be stored (maintained) at any time is termed WM capacity and varies based on the type and characteristics of content that is meant to be retained (Chen et al., 2022). Tasks such as the Sternberg paradigm, in which a series of stimuli are presented, stored, and retrieved, provide an opportunity to distinguish neuroanatomical responses during the stages of encoding, maintenance, and retrieval by allowing these phases of WM to be interrogated separately (Jensen et al., 2002; Sternberg, 1966, 1969). However, distinguishing these phases requires techniques with good temporal precision, as the overall process is frequently completed in just a few seconds.

A collection of neuroimaging studies have used WM tasks such as the Sternberg paradigm to examine the spatiotemporal dynamics of neural oscillatory responses serving each phase of verbal WM processing (Embury et al., 2019; Heinrichs-Graham and Wilson, 2015; Proskovec et al., 2016, 2019a; Rottschy et al., 2012). Robust alpha/beta oscillations have consistently been shown in the occipital cortex during early encoding, with progression towards left frontotemporal cortices throughout later encoding and maintenance phases (Heinrichs-Graham and Wilson, 2015; Proskovec et al., 2016). These responses have often

been implicated in the active processing of visual and verbal stimuli, while activity in regions such as the dorsolateral prefrontal cortex (dlPFC) likely indicates the involvement of executive control in WM (Embury et al., 2019; Heinrichs-Graham and Wilson, 2015; Killanin et al., 2024; Proskovec et al., 2016, 2019a; Rottschy et al., 2012; Wianda and Ross, 2019). Concurrently, sustained alpha/beta oscillatory activity in the left parietal and temporal regions has been observed, which is thought to reflect internal rehearsal of verbal information (i.e., articulatory loop; Heinrichs-Graham and Wilson, 2015; Proskovec et al., 2016, 2019a; Wianda and Ross, 2019; Wilson et al., 2005a, 2005b, 2007). Further, some studies have discerned alpha synchronizations in the parietal and occipital lobes during maintenance, suggesting that alpha activity in some brain regions may facilitate information processing through functional inhibition of incoming visual information (Jensen et al., 2002; Proskovec et al., 2019a; Wianda and Ross, 2019; Wilson et al., 2017). While verbal WM processing is largely left-lateralized across age groups, older adults typically show increased recruitment of right hemispheric prefrontal and temporal cortices, as well as stronger oscillatory activity in left hemispheric homologues (Proskovec et al., 2016; Springer et al., 2023a). Prior research on pediatric populations between 6 and 14 years old has found that some have increased recruitment of the occipitoparietal and cerebellar cortices, but this varies by age and sex, with older youth and females being more likely to display stronger alpha oscillatory activity during maintenance (Embury et al., 2019; Killanin et al., 2024). Other studies using the delayed match-to-sample (DMTS) task have found a similar increase in alpha/-beta oscillatory activity (i.e., decrease from baseline) in the occipital cortex during encoding that dissipates and later increases relative to baseline at the end of maintenance, but this has been shown to be more reduced in older youth and those diagnosed with ADHD (Arjona et al., 2023; Gómez et al., 2023; Lenartowicz et al., 2014, 2019).

Some have posited that WM maintenance operations are susceptible to interference, which can result in a failure to maintain attentional control, as suggested by dual-processing theory (Barrett et al., 2004; Hartshorne and Makovski, 2019). Specifically, dual-processing theory suggests that automatic processing occurs based on past experiences and that goal-directed attention allows for some control over the degree to which automatic processing influences thoughts, feelings, and behaviors (Barrett et al., 2004; Hartshorne and Makovski, 2019). Along those lines, Bonnefond and Jensen (2012) used magnetoencephalography (MEG) to examine the impact of strong versus weak distractors during the maintenance phase of a modified Sternberg WM task. Their analysis focused on posterior alpha responses, which revealed stronger alpha power when participants were anticipating the onset of strong compared to weak distractors, the strength of which correlated with reaction time (Bonnefond and Jensen, 2012). Additionally, they found stronger alpha phase locking prior to the onset of strong versus weak distractors (Bonnefond and Jensen, 2012). Zhou et al. (2023) similarly examined visuospatial WM with auditory and visual distractors to understand if distractor inhibition is modality specific. Their analyses focused on modality specific visual and auditory cortices and they found alpha differences during distractor presentation, with alpha desynchronizations in regions specific to the modality of distractor presentation (i.e., desynchronizations in auditory cortex during auditory distractors and visual cortex during visual distractors; Zhou et al., 2023). In addition, they observed stronger alpha responses during retrieval, which were also modality specific (Zhou et al.,

2023). While these studies provided major advances in our understanding of the impact of distractors in the setting of verbal WM tasks, the impact of sustained distractor presentation at the *whole-brain* level remains to be determined, and this is especially true in regard to the neuronal dynamics supporting WM maintenance operations.

In the current study, we directly examined the impact of visual distractors on verbal WM processing by using both strongly- and weakly-distracting visual stimuli during the maintenance phase of a Sternberg type WM task. Specifically, healthy adults performed a verbal WM task comprised of high-distraction (letters) and low-distraction (pound signs) conditions while undergoing MEG. Consistent with previously described research, we expected robust alpha/beta oscillations during encoding in the occipital and parietal cortices, as well as alpha/beta oscillations during maintenance in the left prefrontal, temporal, and parietal regions. We hypothesized that alpha oscillations in the occipital, parietal, and prefrontal cortices would be stronger in the maintenance phase during the high-compared to low-distraction condition, indicating stronger recruitment of brain regions involved in actively maintaining task-relevant information while ignoring task-irrelevant distractors.

2. Methods

2.1. Participants

Forty-six healthy adults (M_{age}: 27.92, SD_{age}: 4.14, $range_{age}$: 19–35, $N_{female:}$ 28) from the Omaha metropolitan area were enrolled in this study and fully completed the WM paradigm during MEG and underwent a structural MRI. Initial exclusionary criteria included any medical illness affecting central nervous system (CNS) function, neurological or psychiatric disorder, history of head trauma, current substance misuse, and presence of ferromagnetic implanted material. This study protocol was approved by the Boys Town National Research Hospital Institutional Review Board. Written and informed consent was obtained from all participants after a full description of the study was provided.

2.2. Experimental paradigm

Participants performed a visual Sternberg type WM task with distractors during MEG recording (Fig. 1a; Sternberg, 1966). Specifically, they were instructed to fixate on a crosshair presented in the center of the screen. Each trial began with the presentation of an empty 2-by-2 grid with a central fixation cross for 1500 (±350) ms. A grid containing four equally spaced and sized light gray letters was then presented for 1500 ms (encoding). Next, a grid containing four dark gray distractors was displayed for 2500 ms (maintenance). The distractors consisted of either four new letters (high-distraction condition) or four pound signs (low-distraction condition). Finally, a probe containing a single light gray letter was presented in the center of the grid for 1500 ms (retrieval). Participants were instructed to remember the light gray letters, ignore the distractors, and during retrieval, respond with a button press using their right hand to indicate whether the probe letter was included (index finger) or not included (middle finger) in the set of light gray letters. In 50% of trials, the probe letter matched one of the letters displayed during encoding. The high-distraction and low-distraction conditions were presented in a blocked design, with the order being fully

counterbalanced across all participants. Each trial lasted 7000 ms (±350), with a total of 128 trials per condition, resulting in a total run time of approximately 30 min.

2.3. MEG data acquisition

MEG recordings took place in a two-layer VACOSHIELD magnetically-shielded room (Vacuumschmelze, Hanau, Germany). Participants were seated in a non-magnetic chair, with their head positioned within the sensor array. A 306-sensor MEGIN Neo MEG system (Helsinki, Finland) equipped with 204 planar gradiometers and 102 magnetometers was used to sample neuromagnetic responses continuously at 1 kHz with an acquisition bandwidth of 0.1 – 330 Hz. Participants were monitored by a real-time audio-video feed from inside the shielded room throughout MEG data acquisition. Data from each participant were individually corrected for head movement and noise reduced using the signal space separation method with a temporal extension (Taulu and Simola, 2006). For analyses of neural oscillatory responses, only gradiometer data were used (see Sections 2.5 and 2.6).

2.4. Structural MRI processing and MEG coregistration

Prior to MEG recording, five coils were attached to the participant's head and localized, together with the three fiducial points (i.e., nasion, left and right preauriculars) and scalp surface, with a 3D digitizer (Fastrak; Polhemus Navigator Sciences, Colchester, VT). Once the participant was positioned for MEG recording, an electric current with a unique frequency label (e.g., 322 Hz) was fed to each of the coils. This induced a measurable magnetic field and allowed each coil to be localized in reference to the sensors throughout the recording session. Since coil locations were also known in head coordinates, all MEG measurements could be transformed into a common coordinate system. With this coordinate system, each participant's movement-corrected MEG data were co-registered with their structural MRI data prior to source space analyses using BESA MRI (Version 3.0; BESA GmbH, Gräfelfing, Germany). All structural MRI data were acquired on a 3T Siemens Prisma magnet using a 32-channel head coil with the following parameters: TR: 2400 ms; TE: 2.05 ms; field of view: 256 mm; matrix: 256 × 256; slice thickness: 1 mm with no gap; voxel size: 1.0 × 1.0 × 1.0 mm; acquisition plane: sagittal; flip angle: 8°. These anatomical images were aligned parallel to the anterior and posterior commissures and transformed into standardized space. Following source analysis (i. e., beamforming), each participant's 4.0 × 4.0 × 4.0 mm MEG functional images were also transformed into standardized space using the transform that was previously applied to the structural MRI volume and spatially resampled.

2.5. MEG preprocessing, time frequency transformation, and sensor-level statistics

MEG preprocessing and imaging used the Brain Electrical Source Analysis (BESA V7.1) software. Cardiac and eye-blink artifacts were manually removed from the MEG data prior to statistical analysis using signal-space projection (SSP; Uusitalo and Ilmoniemi, 1997). The continuous magnetic time series was divided into epochs of 4000 ms with the onset of encoding stimulus grid defined as 0 ms and the baseline being defined as −550 to −50 ms prior to stimulus onset. Epochs containing artifacts were rejected based on individual amplitude and gradient thresholds. The average amplitude threshold was 1089.55 (*SD* = 313.38) fT/cm and the average gradient threshold was 382.82 (*SD* = 229.62) fT/(cm*ms)

across all participants and conditions. Only trials where participants responded correctly were used for analysis. On average, 91 (SD = 13.16) out of 128 high-distraction and 88 (SD = 14.20) out of 128 low-distraction trials remained after artifact rejection and were used in subsequent analyses. Importantly, the number of trials did not significantly differ between the high- and low-distraction conditions (p = .27).

Artifact-free epochs were transformed into the time-frequency domain using complex demodulation for frequencies from 2–30 Hz with a resolution of 1 Hz and 50 ms, and for frequencies from 30–90 Hz with a resolution of 2 Hz and 25 ms (Kovach and Gander, 2016). These two frequency ranges were transformed separately due to computational limitations and using different resolutions to most appropriately resolve neural responses in each frequency range. The resulting spectral power estimations per sensor were then averaged over trials to generate time-frequency plots of mean spectral density. These sensor-level data were normalized per time-frequency bin using the respective bin's baseline power, which was calculated as the mean power during the −550 ms to −50 ms time period.

The specific time-frequency windows used for imaging were determined by statistical analysis of the sensor-level spectrograms across all participants, trials, and conditions, restricted to the entire array of gradiometers. To reduce the risk of false positive results while maintaining reasonable sensitivity, a two-stage procedure was followed to control for Type I error. In the first stage, paired-samples t-tests against baseline were conducted on each data point and the output spectrogram of t-values was thresholded at $p < .05$ to define time-frequency bins containing potentially significant oscillatory deviations relative to baseline across all participants and conditions. In stage two, time-frequency bins that survived the threshold were clustered with temporally, spectrally, and/or spatially neighboring bins with t-values that were also above the ($p < .05$) threshold, and a cluster value was derived by summing all the t-values of all data points in the cluster. Nonparametric permutation testing was then used to derive a distribution of cluster-values, and the significance level of the observed clusters (from stage 1) were tested directly using this distribution (Ernst, 2004; Maris and Oostenveld, 2007). For each comparison, 5000 permutations were computed to build a distribution of cluster values. Based on these analyses, only the time-frequency windows that contained significant oscillatory events across all trials were subjected to imaging, and these source images were then used to test our hypothesized effects. For a complete description of this methodological approach, see Wiesman and Wilson (2020).

2.6. MEG source imaging and statistics

Cortical responses were imaged through a time-frequency-resolved extension of the linearly constrained minimum variance (LCMV) beamformer (Van Veen et al., 1997; Gross et al., 2001), which applies spatial filters to time-frequency sensor data to calculate voxel-wise source power for the entire brain volume. The single images are derived from the cross-spectral densities of all combinations of MEG gradiometers averaged over the time-frequency range of interest, and the solution of the forward problem for each location on a grid specified by input voxel space. Such images are typically referred to as pseudo-t maps, with units (pseudo-t) that reflect noise-normalized power differences (i.e., active vs. passive) per voxel. Following convention, we computed noise-normalized, source power per voxel

over the entire brain volume in each participant using active (i.e., task) and passive (i. e., baseline) periods of equal duration and bandwidth (Hillebrand et al., 2005) that were based on the statistically determined time-frequency windows from the sensor level analyses. The resulting 3D maps were 4.0 × 4.0 × 4.0 mm resolution and were averaged across all participants and both conditions to assess the anatomical basis of the significant oscillatory responses identified through the sensor-level analysis.

2.7. Statistical analyses

To identify the neuroanatomical basis of distraction inhibition, we performed whole-brain paired-samples *t*-tests (i.e., high-distraction vs. low-distraction) on the beamformer maps per oscillatory response. To correct for multiple comparisons, the resulting images underwent nonparametric permutation testing using a cluster-based permutation method similar to that performed on the sensor-level spectrograms (see Section 2.5), with 5000 permutations per comparison (initial clustering alpha threshold of $p < .005$). On the resulting images, we employed an alpha threshold of $p < .005$, corrected.

3. Results

3.1. Behavioral analysis

Of the 46 enrollees, seven participants were excluded due to low accuracy ($n = 3$), technical difficulties ($n = 1$), and excessive artifacts in their MEG data ($n = 3$). The remaining 39 participants (M_{age}: 28.15, SD_{age}: 3.93, $range_{age}$: 19–35, $N_{female:}$ 23) were included in the final analyses. These participants performed well on the WM task, responding accurately to 93.48% ($SD = 5.42\%$; Fig. 1b) of all trials, with no significant difference in accuracy between high-distraction and low-distraction trials ($t(38) = 1.42$, $p = .16$). Likewise, reaction time did not differ between the high-distraction ($M = 784.71$ ms, $SD = 116.85$ ms) and low-distraction ($M = 783.80$ ms, $SD = 128.61$ ms) conditions ($t(38) = 0.13$ ms, $p = .90$; Fig. 1b).

3.2. Sensor-level analysis

Statistical analysis of sensor-level time-frequency spectrograms, irrespective of condition, revealed significant clusters of theta, alpha, and beta band oscillatory activity (Fig. 2; $p < .001$ corrected). Specifically, theta (3–6 Hz) activity strongly increased relative to baseline immediately following the onset of the encoding grid (i.e., 0 ms) and was sustained throughout encoding and maintenance phases (i.e., 0–4000 ms). Alpha (8–14 Hz) and beta (14–23 Hz) activity strongly decreased relative to baseline shortly after encoding grid onset and continued throughout the encoding and maintenance phases (i.e., 100–3900 ms) in sensors over the left temporal cortex. Additionally, during the maintenance phase, there was a strong early increase in beta activity lasting approximately 500 ms ($\beta_{posterior}$: 12–18 Hz; 2100–2600 ms). Again, all of these clusters were significant after nonparametric permutation tests (i.e., $p < .001$, corrected; Fig. 2). Consistent with previous literature, there was also an increase in alpha power during the maintenance phase, however, this sustained response did not reach statistical significance (Figure S1). Nonetheless, the time-frequency extent of this response overlapped with the significant alpha decrease observed else-where and thus these time-frequency windows were imaged using a whole-brain beamforming

approach. Although our time-frequency spectrograms extended to 90 Hz, there were no significant windows in the gamma range after permutation testing, thus gamma oscillations were not examined in our beamforming analysis as we relied on a data-driven approach.

3.3. Beamformer analysis

To determine the neural regions involved in verbal WM, the sensor-level time-frequency bins described in 3.2 were imaged using a time-frequency-resolved beamformer and the resulting whole-brain maps per neural oscillatory response were averaged across both conditions and all participants (Fig. 3). For the sustained oscillatory responses in theta, we imaged the time windows in non-overlapping 500 ms intervals. Theta (3–6 Hz) oscillatory responses were centered in the visual cortex and largely sustained in this area during encoding and maintenance (Figure S2). For the sustained oscillatory responses in alpha and beta, we imaged the time windows in non-overlapping 350 ms intervals during encoding and the early maintenance period, and 450 ms intervals during maintenance. Alpha (8–14 Hz) oscillatory responses (i.e., decreases relative to the baseline) emerged in the visual cortex during early encoding and gradually progressed to left temporoparietal and frontal cortices during the encoding and maintenance phases (Fig. 3). Finally, beta (β_{full}: 14–23 Hz) oscillatory responses displayed a similar progression with an additional strong increase in power at the onset of the maintenance phase (Fig. 3).

3.4. Condition differences on oscillatory responses

To examine the effects of distraction condition on the neural responses serving WM, the sustained neural responses were averaged across the following time windows per participant to isolate encoding and maintenance operations (theta encoding: 0–1500 ms; alpha encoding: 100–1500 ms; beta encoding [β_{full}: 14–23 Hz]: 100–1500 ms; theta maintenance: 2000–4000 ms; alpha maintenance: 2100–3900 ms; and beta maintenance [β_{full}: 14–23 Hz]: 2100–3900 ms). Separate whole-brain paired *t*-tests were then performed for each of these neural responses, as well as those that were less sustained (theta early maintenance: 1500 – 2000 ms; alpha early maintenance: 1500–1850 ms; beta early maintenance [β_{full}: 14–23 Hz]: 1500–1850; and posterior beta maintenance [$\beta_{posterior}$: 12–18 Hz]: 2100–2600 ms) described above. No significant conditional differences were found for neural responses in the theta band (encoding, early maintenance, and maintenance), the alpha band during encoding and early maintenance, nor the beta band during encoding and posterior maintenance. Beta band neural responses during early maintenance (β_{full}: 14–23 Hz; 1500–1850 ms) showed significant conditional differences in the right inferior frontal gyrus (IFG) and left dorsolateral prefrontal cortex (dlPFC), such that there was stronger beta oscillatory activity (i.e., more negative relative to base-line) during the high- compared to low-distraction condition (Fig. 4; $p < .005$, corrected). During the sustained maintenance responses, there were significant conditional differences in alpha oscillatory activity (8–14 Hz; 2100–3900 ms) in the right middle frontal gyrus (MFG; Fig. 5; $p < .005$, corrected), and in beta oscillatory activity (β_{full}: 14–23 Hz; 2100–3900 ms) in the right anterior prefrontal cortex (PFC; Fig. 5; $p < .005$, corrected). In both cases, the high-distraction condition was associated with stronger alpha (right MFG) and beta (anterior PFC) oscillations compared to the low distraction condition (i.e., more negative relative to baseline in the high-distraction condition).

3. Discussion

In the current study, we investigated the oscillatory dynamics supporting WM encoding and maintenance in healthy adults using a Sternberg type WM task with high- and low-level distractors. Slightly after the presentation of the encoding grid, we observed a sustained decrease in both alpha (8–14 Hz) and beta (β_{full}; 14–23 Hz) power relative to baseline across both conditions. These sustained decreases in alpha and beta began bilaterally in the occipital cortex and spread anterior along the left hemisphere to the temporoparietal and frontal cortices before dissipating in the latter half of maintenance. In addition, we found a sustained increase in theta (3–6 Hz) power throughout the encoding and maintenance periods, while beta power increased briefly relative to baseline during early maintenance ($\beta_{posterior}$; 12–18 Hz). While we did not observe conditional differences in accuracy or reaction time, we identified a series of oscillatory differences (i.e., high vs. low distractors) in brain regions critical for WM processing. Whole-brain paired *t*-tests revealed stronger alpha and beta oscillatory activity (i.e., more negative relative to baseline) during the high- relative to the low-distraction condition in right prefrontal regions during the maintenance period. Specifically, beta oscillations in the left dlPFC and right IFG during early maintenance were stronger in the high-distraction relative to the low-distraction condition. Similarly, during the sustained maintenance response, alpha oscillations in the right MFG and beta oscillations in the right anterior PFC were stronger (i.e., more negative relative to baseline) during the high-distraction relative to the low-distraction condition. These findings support prior research showing sustained decreases relative to baseline in alpha and beta activity following the onset of visual and verbal stimuli in both MEG and EEG and reinforces the view that WM processes are supported by complex widespread temporal dynamics (Gómez et al., 2024; Heinrichs-Graham and Wilson, 2015; Proskovec et al., 2016, 2019a). Conversely, our findings did not support previous work indicating that posterior alpha oscillations were modulated by distractor condition or that distractor load impacted reaction time (Bonnefond and Jensen, 2012). Below, we discuss the implications of these findings for understanding the impact of distractors on the neural oscillations serving verbal WM.

Our overarching finding is that bilateral regions of the PFC are critical to suppressing distractors in the context of WM processing. The PFC is known to receive inputs from cortical and subcortical structures and to communicate this information within the PFC and to external regions (Miller and Cohen, 2001). Like controlled attention, this top-down processing is thought to mitigate the effects of interference by distractors and is influenced by WM capacity (Barrett et al., 2004; Miller and Cohen, 2001). Indeed, individuals with high WM capacity are better able to inhibit task-irrelevant information and have greater activation changes in the PFC when completing a WM task, suggesting that the PFC is centrally involved in maintaining WM representations and inhibiting task-irrelevant information (Hu et al., 2019; Mecklinger et al., 2003; Sakai et al., 2002; Wager et al., 2014), which is fully consistent with our current findings. Additionally, Wager et al. (2014) found that specific regions of the frontal and prefrontal cortices predicted verbal WM task performance in the context of distractors, no-distractors, or both conditions, with both dorsolateral and ventrolateral prefrontal cortices having subregions that predicted only no-

distractor or both conditions. Our results implicate beta activity in the right anterior PFC and left dlPFC in functional inhibition of distractors, which corroborates previous findings regarding the role of the PFC in WM and distractor inhibition.

In addition to the PFC, the IFG and MFG have been implicated in inhibitory control, reactive processes, and attention reorienting (Corbetta et al., 2008; Gavazzi et al., 2021). The IFG and PFC are considered part of the ventral attention network (VAN) and are thought to be activated alongside the dorsal attention network (DAN) when attention reorienting is necessary (Corbetta et al., 2008). Specifically, the VAN is composed of a right-lateralized network including the temporoparietal junction (TPJ), IFG, and MFG (Corbetta et al., 2008; Doricchi et al., 2010). Contrary to the TPJ, which is typically involved in attention regardless of predictability, the IFG and MFG are more active when something unexpected occurs and attention reorienting is necessary (Doricchi et al., 2010; Shulman et al., 2009). Further, the right MFG is a functional hub for attentional control that is activated when viewing distractors, especially incongruent distractors, and may be implicated in reactive control and inhibition of distractors during cognitive as well as motor tasks (Corbetta et al., 2008; Marini et al., 2016). Thus, the right MFG is thought to play a critical role in distractor-filtering during attentional control tasks (Marini et al., 2016). In the current study, we indeed see stronger alpha/beta oscillatory activity in the right MFG and IFG during the high- compared to low-distraction condition, supporting the idea that the VAN suppresses distracting information and allows attention to be redirected. Our results also extend these findings by providing insight on the key spectral windows for these neural responses.

Importantly, high- compared to low-distraction elicited stronger alpha (8–14 Hz) oscillatory activity (i.e., more negative relative to baseline) during maintenance and stronger beta (β_{full}; 14–23 Hz) oscillations during both the early and extended maintenance periods in prefrontal regions, including the right MFG, right anterior PFC, right IFG, and left dlPFC. These results underscore the importance of alpha/beta activity in inhibiting distracting information and support prior research on the role of alpha in functional inhibition (Bonnefond and Jensen, 2012; Jensen and Mazaheri, 2010; Roux and Uhlhaas, 2014; Zhou et al., 2023). For example, EEG work using a DMTS spatial working memory task has showed weaker decreases in alpha power during encoding in children with ADHD compared to typically developing youth, across low and high load trials (Lenartowicz et al., 2014, 2019). Such reduced alpha responses also correlated with ADHD symptomatology, as well as reading comprehension and executive function scores, all of which corroborate the theory that alpha/beta activity during the encoding window is critical for attentional control and functional inhibition (Lenartowicz et al., 2014, 2019). Specifically, our results support prior research which showed that alpha oscillations vary based on the strength of the distracting information (Bonnefond and Jensen, 2012). However, contrary to these findings, we did not observe differences in alpha oscillatory activity in the occipitotemporal area; rather, our results were limited to prefrontal regions. Note that this difference was not due to the fact that the posterior alpha increase did not reach significance in our sensor level statistical analysis, as the band surrounding the response was imaged at the whole-brain anyway due to the strength of the alpha decrease at the same time in temporal cortices. It is possible that this is due to differences in sample demographics, as studies investigating aging have shown that posterior alpha activity during maintenance varies with age (Proskovec et al., 2016).

While the mean age of our sample was similar to that of Bonnefond and Jensen (2012), the two samples differed in other important ways, including the final sample of the current study being twice as large and near equally split by sex, while that of Bonnefond and Jensen was about 90% female. Future studies should examine whether the strength of such posterior alpha responses is affected by sex differences and/or probe possible interactions with aging.

In contrast to alpha, far fewer studies have discussed the role of beta oscillatory activity in WM. Previous research has identified age- and load-related differences in WM in a frequency range between 9–16 Hz, inclusive of both alpha and beta oscillatory activity (Proskovec et al., 2016, 2019a). Additionally, visuospatial WM tasks are known to involve both beta and gamma oscillatory activity, with beta occurring in ventral areas related to color processing and in visual areas related to location processing (Honkanen et al., 2015; Proskovec et al., 2018). This suggests that beta oscillations may play a role in feature-specific WM maintenance, which may explain why prior research has been mixed in regards to the role of beta oscillatory activity in WM. Recent work has also linked beta oscillations to the inhibition of a variety of higher order processes (Castiglione et al., 2019; Pavlov and Kotchoubey, 2021; Schmidt et al., 2019; Wagner et al., 2018; Zavala et al., 2017; 2018). For example, studies have shown that halting retrieval in think/no-think tasks is associated with right frontal beta activity, especially when an individual successfully halts retrieval (Castiglione et al., 2019). Similarly, beta oscillations (i.e., decreases relative to baseline) in the medial PFC have been shown during go/no-go tasks when a conflict is displayed (e.g., a red arrow pointing right and participants must respond by pressing the left button) and the individual is successful in adapting their response (Zavala et al., 2018). Finally, a recent study showed that beta oscillations are stronger when manipulating a memory is required over just maintaining it (Pavlov and Kotchoubey, 2021). These findings, in addition to the results of the current study, suggest that beta oscillatory activity in the PFC is involved in many higher order cognitive processes including WM, controlled attention, and cognitive control (Lundqvist et al., 2024; Zavala et al., 2018).

Although we had many statistically significant alpha and beta findings, this was not the case for theta activity. While theta (3–6 Hz) activity increased for a sustained period throughout encoding and maintenance, no differences were identified between task conditions at the source level. Current literature in WM is mixed in regards to theta, with many studies reporting significant theta oscillatory activity (Brookes et al., 2011; Jensen and Tesche, 2002; McDermott, et al., 2016a; Onton et al., 2005; Proskovec et al., 2019a), while others do not despite using similar or identical tasks (Embury et al., 2018; McDermott et al., 2016b; Proskovec et al., 2016; Wiesman et al., 2016). Additionally, theta has not previously been found to differ in tasks that use distractor presentation and thus when observed may be related to the encoding and maintenance of WM, but not to functional inhibition (Roux and Uhlhaas, 2014). Together, these mixed results necessitate further investigation of the role of theta in WM processes and functional inhibition.

While it was not the focus of our study, it should be noted that we found no differences in accuracy or reaction time between conditions. Similarly, Bonnefond and Jensen (2012) did not observe conditional differences in accuracy, however they found a difference in reaction time. These results may differ due to having a larger sample with different demographics,

though they may also be attributed to differences in task design. Bonnefond and Jensen (2012) showed a series of single letters and symbols one after the other, while our task displayed sets of 4 letters/symbols. It may be the case that less WM capacity was required to maintain this information, and thus this task may not elicit some of the same behavioral differences found in other WM studies.

Although this study contributes much to our understanding of the neurophysiological responses underlying WM in healthy adults, it is not without limitations. First, due to our use of a blocked design, the type of distractor was predictable and thus our results may not generalize to task designs that use unpredictable distractors. Second, some may consider this to be a short-term visual memory task as opposed to a traditional WM task requiring cognitive operations or manipulation of the stimulus set. Although the task requires participants to maintain task-relevant information while actively inhibiting visual distractors, which seemingly qualifies as a WM paradigm, and our neural results concur with prior literature on WM, we believe it is important to acknowledge this distinction as a potential limitation. Third, as is true of many forms of time-frequency transformation, it is possible that a spread of power, especially in lower frequencies, from early stimulus processing to our baseline could have biased these results. However, this would bias against finding significant task-related neural activity in the lower frequency bands (i.e., theta) and we did indeed identify responses in this band. Further, since our contrast of interest was the conditional comparison, and both conditions would be biased equally in this sense, this would not impact conditional differences presented here. Fourth, we focused on the impact of distractor type on verbal WM processing and our results should not be generalized to spatial WM processing, as the key oscillatory responses differ considerably (Proskovec et al., 2018, 2019b). Future work should examine the impact of distractor type on spatial WM specifically. Finally, our sample was comprised of healthy young adults between the ages of 19 and 35 and future work should examine aging and groups with neurological and/or psychiatric disorders, as it is possible that those with WM deficits could be much more susceptible to distractors (Arif et al., 2024; Embury et al., 2023; Killanin et al., 2022; Springer et al., 2023b). Thus, although the current study contributes substantially to our understanding of WM processes in the healthy brain, much work remains to fully understand how distractors can influence WM processing.

In conclusion, the present study utilized advanced MEG imaging of neural oscillatory activity to examine the impact of visual distractors on verbal WM processing. Novel aspects of the study included using a sustained distractor presentation approach and data-driven whole-brain analyses. Our key results indicated that alpha/beta oscillatory activity plays a major role in the inhibition of distracting information during WM maintenance. These findings uphold and extend prior research and provide valuable new insight into the neurophysiological processes underlying functional inhibition and cognitive control during verbal WM processing in healthy young adults.

Supplementary Material

Refer to Web version on PubMed Central for supplementary material.

Funding

This study was supported by the National Institutes of Health through grants R01-MH116782 (TWW), R01-MH118013 (TWW), R01-DA047828 (TWW), R01-DA056223 (TWW), P20-GM144641 (TWW and EHG), and S10-OD028751 (TWW and EHG). The funders had no role in the study design, collection, analysis, or interpretation of data, nor did they influence writing the report or the decision to submit this work for publication.

References

Arif Y, Killanin AD, Zhu J, Willett MP, Okelberry HJ, Johnson HJ, Wilson TW, 2024. Hypertension impacts the oscillatory dynamics serving the encoding phase of verbal working memory. Hypertension 81 (7), 1609–1618. 10.1161/HYPERTENSIONAHA.124.22698. [PubMed: 38690668]

Arjona A, Angulo-Ruiz BY, Rodríguez-Martínez EI, Cabello-Navarro C, Gómez CM, 2023. Time-frequency neural dynamics of ADHD children and adolescents during a working memory task. Neurosci. Lett 798, 137100. 10.1016/j.neulet.2023.137100. [PubMed: 36720344]

Baddeley A, 1992. Working memory. Science 255 (5044), 556–559. 10.1126/science.1736359. [PubMed: 1736359]

Baddeley AD, 1983. Working memory. Philos. Trans. R. Soc. Lond., B, Biol. Sci 302 (1110), 311–324. https://www.jstor.org/stable/2395996.

Barrett LF, Tugade MM, Engle RW, 2004. Individual differences in working memory capacity and dual-process theories of the mind. Psychol. Bull 130 (4), 553–573. 10.1037/0033-2909.130.4.553. [PubMed: 15250813]

Bonnefond M, Jensen O, 2012. Alpha oscillations serve to protect working memory maintenance against anticipated distracters. Curr. Biol 22 (20), 1969–1974. 10.1016/j.cub.2012.08.029. [PubMed: 23041197]

Brookes MJ, Wood JR, Stevenson CM, Zumer JM, White TP, Liddle PF, Morris PG, 2011. Changes in brain network activity during working memory tasks: a magnetoencephalography study. Neuroimage 55 (4), 1804–1815. 10.1016/j.neuroimage.2010.10.074. [PubMed: 21044687]

Castiglione A, Wagner J, Anderson M, Aron AR, 2019. Preventing a thought from coming to mind elicits increased right frontal beta just as stopping action does. Cereb. Cortex 29 (5), 2160–2172. 10.1093/cercor/bhz017. [PubMed: 30806454]

Chen Y-T, van Ede F, Kuo B-C, 2022. Alpha oscillations track content-specific working memory capacity. J. Neurosci 42 (38), 7285–7293. 10.1523/JNEUROSCI.2296-21.2022. [PubMed: 35995565]

Corbetta M, Patel G, Shulman GL, 2008. The reorienting system of the human brain: from environment to theory of mind. Neuron 58 (3), 306–324. 10.1016/j.neuron.2008.04.017. [PubMed: 18466742]

D'Esposito M, Postle BR, 2015. The cognitive neuroscience of working memory. Annu. Rev. Psychol 66 (1), 115–142. 10.1146/annurev-psych-010814-015031. [PubMed: 25251486]

Doricchi F, Macci E, Silvetti M, Macaluso E, 2010. Neural correlates of the spatial and expectancy components of endogenous and stimulus-driven orienting of attention in the Posner task. Cereb. Cortex 20 (7), 1574–1585. 10.1093/cercor/bhp215. [PubMed: 19846472]

Embury CM, Lord GH, Drincic AT, Desouza CV, Wilson TW, 2023. Glycemic control level alters working memory neural dynamics in adults with type 2 diabetes. Cereb. Cortex 33 (13), 8333–8341. 10.1093/cercor/bhad119. [PubMed: 37005060]

Embury CM, Wiesman AI, Proskovec AL, Heinrichs-Graham E, McDermott TJ, Lord GH, Brau KL, Drincic AT, Desouza CV, Wilson TW, 2018. Altered brain dynamics in patients with type 1 diabetes during working memory processing. Diabetes 67 (6), 1140–1148. 10.2337/db17-1382. [PubMed: 29531139]

Embury CM, Wiesman AI, Proskovec AL, Mills M, Heinrichs-Graham E, Wang Y-P, Calhoun VD, Stephen JM, Wilson TW, 2019. Neural dynamics of verbal working memory processing in children and adolescents. Neuroimage 185, 191–197. 10.1016/j.neuroimage.2018.10.038. [PubMed: 30336254]

Ernst MD, 2004. Permutation Methods: A Basis for Exact Inference. Stat. Sci 19 (4), 676–685. 10.1214/088342304000000396.

Gavazzi G, Giovannelli F, Currò T, Mascalchi M, Viggiano MP, 2021. Contiguity of proactive and reactive inhibitory brain areas: a cognitive model based on ALE meta-analyses. Brain Imaging Behav. 15 (4), 2199–2214. 10.1007/s11682-020-00369-5. [PubMed: 32748318]

Gómez CM, Linares R, Rodríguez-Martínez EI, Pelegrina S, 2024. Age-related changes in brain oscillatory patterns during an n-back task in children and adolescents. Int. J. Psychophysiol 202, 112372. 10.1016/j.ijpsycho.2024.112372. [PubMed: 38849088]

Gómez CM, Muñoz V, Rodríguez-Martínez EI, Arjona A, Barriga-Paulino CI, Pelegrina S, 2023. Child and adolescent development of the brain oscillatory activity during a working memory task. Brain Cogn. 167, 105969. 10.1016/j.bandc.2023.105969. [PubMed: 36958141]

Gross J, Kujala J, Hamalainen M, Timmermann L, Schnitzler A, Salmelin R, 2001. Dynamic imaging of coherent sources: Studying neural interactions in the human brain. Proceedings of the National Academy of Sciences of the United States of America 98 (2). 10.1073/pnas.98.2.694.

Hartshorne JK, Makovski T, 2019. The effect of working memory maintenance on long-term memory. Mem. Cognit 47 (4), 749–763. 10.3758/s13421-019-00908-6.

Heinrichs-Graham E, Wilson TW, 2015. Spatiotemporal oscillatory dynamics during the encoding and maintenance phases of a visual working memory task. Cortex 69, 121–130. 10.1016/j.cortex.2015.04.022. [PubMed: 26043156]

Hillebrand A, Singh KD, Holliday IE, Furlong PL, Barnes GR, 2005. A new approach to neuroimaging with magnetoencephalography. Hum. Brain Mapp 25 (2), 199–211. 10.1002/hbm.20102. [PubMed: 15846771]

Honkanen R, Rouhinen S, Wang SH, Palva JM, Palva S, 2015. Gamma oscillations underlie the maintenance of feature-specific information and the contents of visual working memory. Cereb. Cortex 25 (10), 3788–3801. 10.1093/cercor/bhu263. [PubMed: 25405942]

Hu Z, Barkley CM, Marino SE, Wang C, Rajan A, Bo K, Samuel IBH, Ding M, 2019. Working memory capacity is negatively associated with memory load modulation of alpha oscillations in retention of verbal working memory. J. Cogn. Neurosci 31 (12), 1933–1945. 10.1162/jocn_a_01461. [PubMed: 31418335]

Jensen O, Gelfand J, Kounios J, Lisman JE, 2002. Oscillations in the alpha band (9–12 Hz) increase with memory load during retention in a short-term memory task. Cereb. Cortex 12 (8), 877–882. 10.1093/cercor/12.8.877. [PubMed: 12122036]

Jensen O, Mazaheri A, 2010. Shaping functional architecture by oscillatory alpha activity: gating by inhibition. Front. Hum. Neurosci 4. 10.3389/fnhum.2010.00186.

Jensen O, Tesche CD, 2002. Frontal theta activity in humans increases with memory load in a working memory task. Eur. J. Neurosci 15 (8), 1395–1399. 10.1046/j.1460-9568.2002.01975.x. [PubMed: 11994134]

Killanin AD, Embury CM, Picci G, Heinrichs-Graham E, Wang Y-P, Calhoun VD, Stephen JM, Wilson TW, 2022. Trauma moderates the development of the oscillatory dynamics serving working memory in a sex-specific manner. Cereb. Cortex 32 (22), 5206–5215. 10.1093/cercor/bhac008. [PubMed: 35106552]

Killanin AD, Ward TW, Embury CM, Calhoun VD, Wang Y-P, Stephen JM, Picci G, Heinrichs-Graham E, Wilson TW, 2024. Better with age: developmental changes in oscillatory activity during verbal working memory encoding and maintenance. Dev. Cogn. Neurosci 66, 101354. 10.1016/j.dcn.2024.101354. [PubMed: 38330526]

Kovach CK, Gander PE, 2016. The demodulated band transform. J. Neurosci. Methods 261, 135–154. 10.1016/j.jneumeth.2015.12.004. [PubMed: 26711370]

Lenartowicz A, Delorme A, Walshaw PD, Cho AL, Bilder RM, McGough JJ, McCracken JT, Makeig S, Loo SK, 2014. Electroencephalography correlates of spatial working memory deficits in attention-deficit/hyperactivity disorder: vigilance, encoding, and maintenance. J. Neurosci 34 (4), 1171–1182. 10.1523/JNEUROSCI.1765-13.2014. [PubMed: 24453310]

Lenartowicz A, Truong H, Salgari GC, Bilder RM, McGough J, McCracken JT, Loo SK, 2019. Alpha modulation during working memory encoding predicts neurocognitive impairment in ADHD. J. Child Psychol. Psychiatry 60 (8), 917–926. 10.1111/jcpp.13042. [PubMed: 30883769]

Lundqvist M, Miller EK, Nordmark J, Liljefors J, Herman P, 2024. Beta: bursts of cognition. Trends Cogn. Sci. (Regul. Ed.) 10.1016/j.tics.2024.03.010.

Marini F, Demeter E, Roberts KC, Chelazzi L, Woldorff MG, 2016. Orchestrating proactive and reactive mechanisms for filtering distracting information: brain-behavior relationships revealed by a mixed-design fMRI study. J. Neurosci 36 (3), 988–1000. 10.1523/JNEUROSCI.2966-15.2016. [PubMed: 26791226]

Maris E, Oostenveld R, 2007. Nonparametric statistical testing of EEG- and MEG-data. J. Neurosci. Methods 164 (1), 177–190. 10.1016/j.jneumeth.2007.03.024. [PubMed: 17517438]

McDermott TJ, Badura-Brack AS, Becker KM, Ryan TJ, Bar-Haim Y, Pine DS, Khanna MM, Heinrichs-Graham E, Wilson TW, 2016a. Attention training improves aberrant neural dynamics during working memory processing in veterans with PTSD. Cognit. Affect. Behav. Neurosci 16 (6), 1140–1149. 10.3758/s13415-016-0459-7. [PubMed: 27722837]

McDermott TJ, Badura-Brack AS, Becker KM, Ryan TJ, Khanna MM, Heinrichs-Graham E, Wilson TW, 2016b. Male veterans with PTSD exhibit aberrant neural dynamics during working memory processing: an MEG study. J. Psychiatry Neurosci 41 (4), 251–260. 10.1503/jpn.150058. [PubMed: 26645740]

Mecklinger A, Weber K, Gunter TC, Engle RW, 2003. Dissociable brain mechanisms for inhibitory control: effects of interference content and working memory capacity. Cognit. Brain Res 18 (1), 26–38. 10.1016/j.cogbrainres.2003.08.008.

Miller EK, Cohen JD, 2001. An integrative theory of prefrontal cortex function. Annu. Rev. Neurosci 24 (1), 167–202. 10.1146/annurev.neuro.24.1.167. [PubMed: 11283309]

Onton J, Delorme A, Makeig S, 2005. Frontal midline EEG dynamics during working memory. Neuroimage 27 (2), 341–356. 10.1016/j.neuroimage.2005.04.014. [PubMed: 15927487]

Pavlov YG, Kotchoubey B, 2021. Temporally distinct oscillatory codes of retention and manipulation of verbal working memory. Eur. J. Neurosci 54 (7), 6497–6511. 10.1111/ejn.15457. [PubMed: 34514642]

Proskovec AL, Heinrichs-Graham E, Wilson TW, 2016. Aging modulates the oscillatory dynamics underlying successful working memory encoding and maintenance. Hum. Brain Mapp 37 (6), 2348–2361. 10.1002/hbm.23178. [PubMed: 26991358]

Proskovec AL, Heinrichs-Graham E, Wilson TW, 2019a. Load modulates the alpha and beta oscillatory dynamics serving verbal working memory. Neuroimage 184, 256–265. 10.1016/j.neuroimage.2018.09.022. [PubMed: 30213775]

Proskovec AL, Wiesman AI, Heinrichs-Graham E, Wilson TW, 2018. Beta oscillatory dynamics in the prefrontal and superior temporal cortices predict spatial working memory performance. Sci. Rep 8 (1), 8488. 10.1038/s41598-018-26863-x. [PubMed: 29855522]

Proskovec AL, Wiesman AI, Heinrichs-Graham E, Wilson TW, 2019b. Load effects on spatial working memory performance are linked to distributed alpha and beta oscillations. Hum. Brain Mapp 40 (12), 3682–3689. 10.1002/hbm.24625. [PubMed: 31077487]

Rottschy C, Langner R, Dogan I, Reetz K, Laird AR, Schulz JB, Fox PT, Eickhoff SB, 2012. Modelling neural correlates of working memory: a coordinate-based meta-analysis. Neuroimage 60 (1), 830–846. 10.1016/j.neuroimage.2011.11.050. [PubMed: 22178808]

Roux F, Uhlhaas PJ, 2014. Working memory and neural oscillations: alpha–gamma versus theta–gamma codes for distinct WM information? Trends Cogn. Sci. (Regul. Ed.) 18 (1), 16–25. 10.1016/j.tics.2013.10.010.

Sakai K, Rowe JB, Passingham RE, 2002. Active maintenance in prefrontal area 46 creates distractor-resistant memory. Nat. Neurosci 5 (5), 479–484. 10.1038/nn846. [PubMed: 11953754]

Schmidt R, Ruiz MH, Kilavik BE, Lundqvist M, Starr PA, Aron AR, 2019. Beta oscillations in working memory, executive control of movement and thought, and sensorimotor function. J. Neurosci 39 (42), 8231–8238. 10.1523/JNEUROSCI.1163-19.2019. [PubMed: 31619492]

Shulman GL, Astafiev SV, Franke D, Pope DLW, Snyder AZ, McAvoy MP, Corbetta M, 2009. Interaction of stimulus-driven reorienting and expectation in ventral and dorsal frontoparietal and basal ganglia-cortical networks. J. Neurosci 29 (14), 4392–4407. 10.1523/JNEUROSCI.5609-08.2009. [PubMed: 19357267]

Springer SD, Okelberry HJ, Willett MP, Johnson HJ, Meehan CE, Schantell M, Embury CM, Rempe MP, Wilson TW, 2023a. Age-related alterations in the oscillatory dynamics serving verbal working memory processing. Aging 15 (24), 14574–14590. 10.18632/aging.205403. [PubMed: 38154102]

Springer SD, Okelberry HJ, Willett MP, Johnson HJ, Meehan CE, Schantell M, Embury CM, Rempe MP, Wilson TW, 2023b. Age-related alterations in the oscillatory dynamics serving verbal working memory processing. Aging 15 (24), 14574–14590. 10.18632/aging.205403. [PubMed: 38154102]

Sternberg S, 1966. High-Speed scanning in human memory. Science 153 (3736), 652–654. 10.1126/science.153.3736.652. [PubMed: 5939936]

Sternberg S, 1969. Memory-Scanning: mental processes revealed by reaction-time experiments. Am. Sci 57 (4), 421–457. http://www.jstor.org/stable/27828738. [PubMed: 5360276]

Taulu S, Simola J, 2006. Spatiotemporal signal space separation method for rejecting nearby interference in MEG measurements. Phys. Med. Biol 51, 1759–1768. 10.1088/0031-9155/51/7/008. [PubMed: 16552102]

Uusitalo MA, Ilmoniemi RJ, 1997. Signal-space projection method for separating MEG or EEG into components. Med. Biol. Eng. Comput 35 (2), 135–140. 10.1007/BF02534144. [PubMed: 9136207]

Van Veen BD, Van Drongelen W, Yuchtman M, Suzuki A, 1997. Localization of brain electrical activity via linearly constrained minimum variance spatial filtering. IEEE Transactions on Biomedical Engineering 44 (9), 867–880. 10.1109/10.623056. [PubMed: 9282479]

Wager TD, Spicer J, Insler R, Smith EE, 2014. The neural bases of distracter-resistant working memory. Cognit. Affect. Behav. Neurosci 14 (1), 90–105. 10.3758/s13415-013-0226-y. [PubMed: 24366656]

Wagner J, Wessel JR, Ghahremani A, Aron AR, 2018. Establishing a right frontal beta signature for stopping action in scalp EEG: implications for Testing inhibitory control in other task contexts. J. Cogn. Neurosci 30 (1), 107–118. 10.1162/jocn_a_01183. [PubMed: 28880766]

Wianda E, Ross B, 2019. The roles of alpha oscillation in working memory retention. Brain Behav. 9 (4), e01263. 10.1002/brb3.1263. [PubMed: 30887701]

Wiesman AI, Heinrichs-Graham E, McDermott TJ, Santamaria PM, Gendelman HE, Wilson TW, 2016. Quiet connections: reduced fronto-temporal connectivity in nondemented Parkinson's Disease during working memory encoding. Hum. Brain Mapp 37 (9), 3224–3235. 10.1002/hbm.23237. [PubMed: 27151624]

Wiesman AI, Wilson TW, 2020. Attention modulates the gating of primary somatosensory oscillations. Neuroimage 211, 116610. 10.1016/j.neuroimage.2020.116610. [PubMed: 32044438]

Wilson TW, Leuthold AC, Lewis SM, Georgopoulos AP, Pardo PJ, 2005a. Cognitive dimensions of orthographic stimuli affect occipitotemporal dynamics. Exp. Brain Res 167 (2), 141–147. 10.1007/s00221-005-0011-4. [PubMed: 16096785]

Wilson TW, Leuthold AC, Lewis SM, Georgopoulos AP, Pardo PJ, 2005b. The time and space of lexicality: a neuromagnetic view. Exp. Brain Res 162 (1), 1–13. 10.1007/s00221-004-2099-3. [PubMed: 15517213]

Wilson TW, Leuthold AC, Moran JE, Pardo PJ, Lewis SM, Georgopoulos AP, 2007. Reading in a deep orthography: neuromagnetic evidence for dual-mechanisms. Exp. Brain Res 180 (2), 247. 10.1007/s00221-007-0852-0. [PubMed: 17256164]

Wilson TW, Proskovec AL, Heinrichs-Graham E, O'Neill J, Robertson KR, Fox HS, Swindells S, 2017. Aberrant neuronal dynamics during working memory operations in the aging HIV-infected brain. Sci. Rep 7 (1), 41568. 10.1038/srep41568. [PubMed: 28155864]

Woodman GF, Vogel EK, 2005. Fractionating working memory. Psychol. Sci 16 (2), 106–113. 10.1111/j.0956-7976.2005.00790.x. [PubMed: 15686576]

Zavala BA, Jang AI, Zaghloul KA, 2017. Human subthalamic nucleus activity during non-motor decision making. Elife 6. 10.7554/eLife.31007.

Zavala B, Jang A, Trotta M, Lungu CI, Brown P, Zaghloul KA, 2018. Cognitive control involves theta power within trials and beta power across trials in the prefrontal-subthalamic network. Brain 141 (12), 3361–3376. 10.1093/brain/awy266. [PubMed: 30358821]

Zhou YJ, Ramchandran A, Haegens S, 2023. Alpha oscillations protect working memory against distracters in a modality-specific way. Neuroimage 278, 120290. 10.1016/j.neuroimage.2023.120290. [PubMed: 37482324]

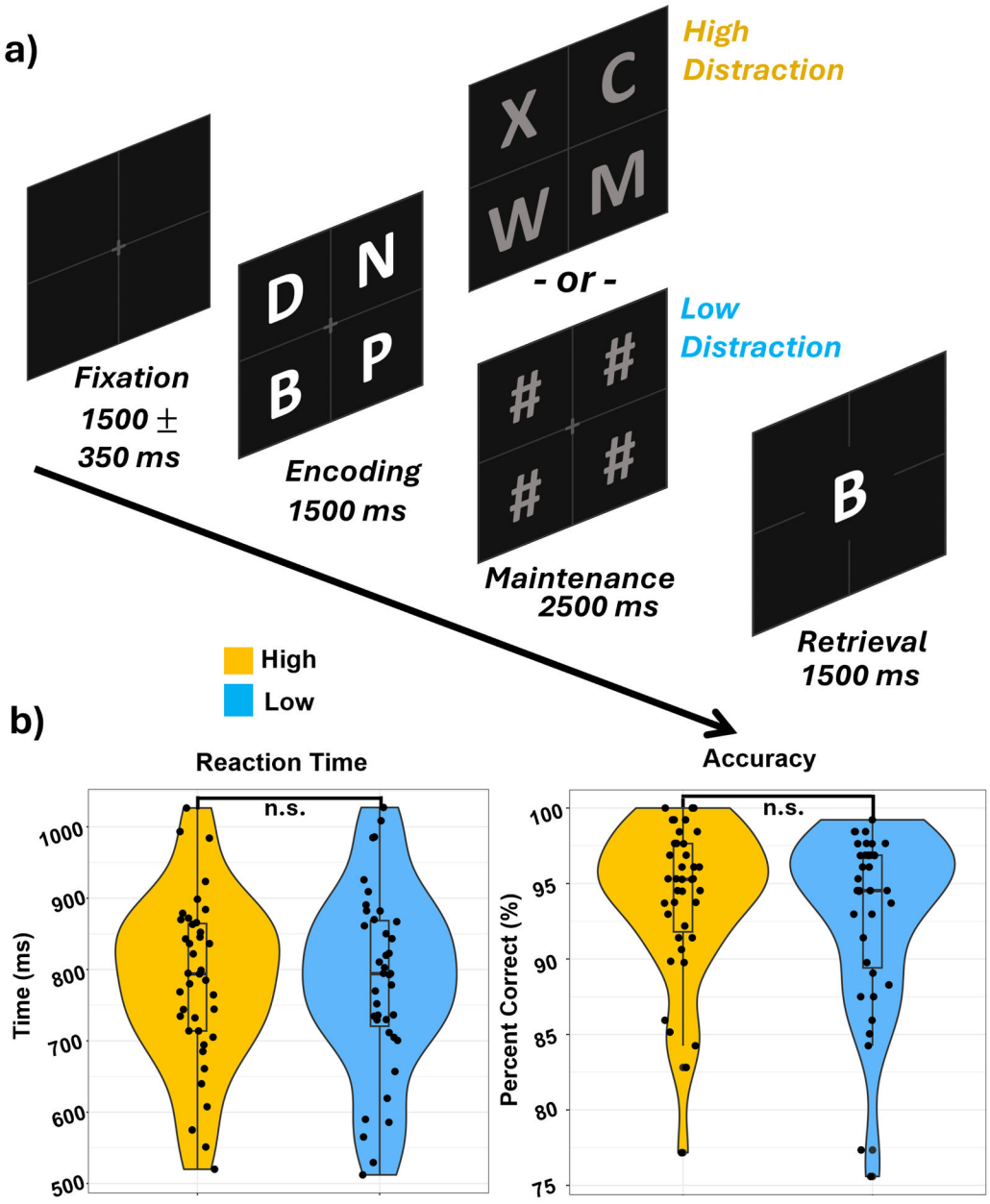

Fig. 1. Verbal Working Memory Paradigm and Behavior.

A) Each trial started with an empty 2-by-2 grid with a central fixation cross for 1500 (± 350) ms followed by the appearance of four letters within the grid for 1500 ms (encoding), which were replaced by four distractors in the form of either letters (high-distraction) or pound signs (low-distraction) for 2500 ms (maintenance). Finally, a probe letter in the center of the grid appeared for 1500 ms (retrieval) and participants were instructed to respond with a button press as to whether the probe letter was present or absent in the initial encoding set of four letters. B) Reaction time (left) and accuracy (right) did not statistically differ between conditions.

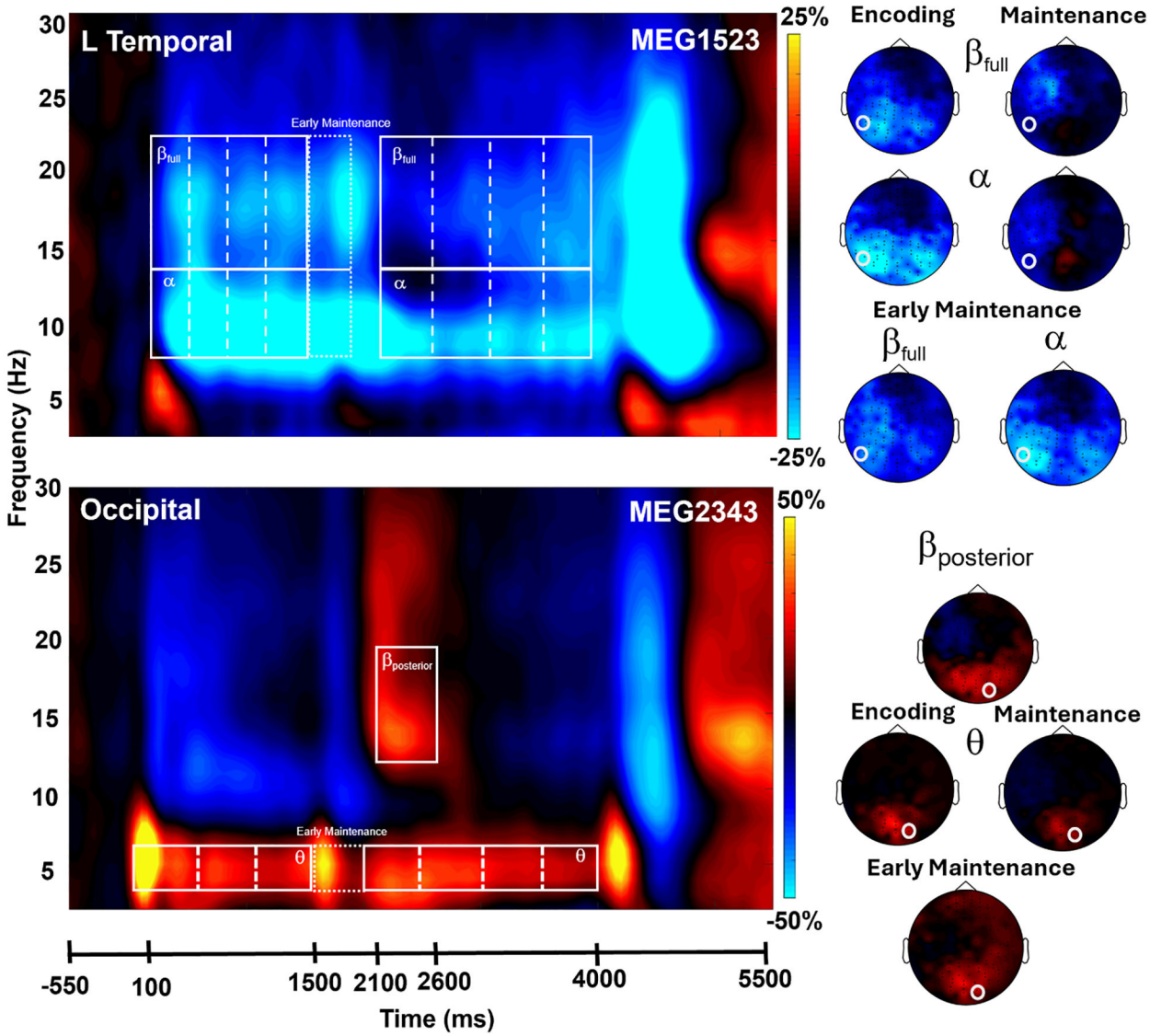

Fig. 2. Sensor-level analysis of oscillatory responses.

MEG time-frequency spectrograms with time (ms) on the x-axis and frequency (Hz) on the y-axis. The onset of the encoding grid occurred at 0 ms. Power is shown in percent change units relative to the baseline period (−550 to −50 ms). Data has been averaged across all trials and all participants in both the high-distraction and low-distraction conditions. Top panel: Sustained decreases in the alpha (8–14 Hz) and beta (β_{full}: 14–23 Hz) spectral bands were observed near left frontal and temporal sensors. Bottom panel: Increases in the theta (3–6 Hz) and posterior beta ($\beta_{posterior}$: 12–18 Hz) range were observed in sensors near the occipital cortex. White boxes denote the time-frequency windows used for source-space analyses. These time-frequency windows were statistically significant ($p < .001$, corrected) in the sensor level analyses. Right: 2D topographical maps were computed for each oscillatory response window. Note that these have been averaged across time windows comprising the extended encoding and maintenance responses in alpha, beta, and theta. The white circles mark the location of the sensors displayed in each spectrogram.

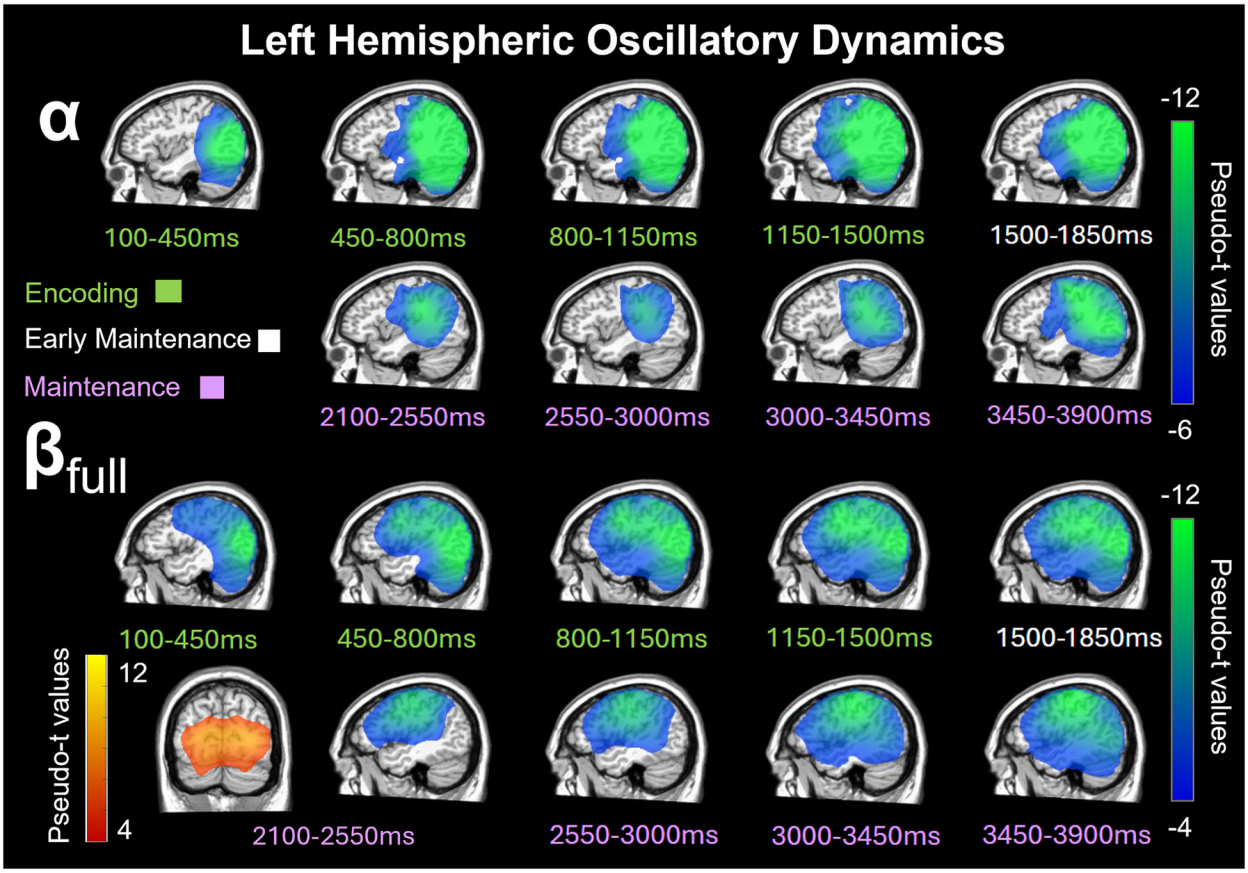

Fig. 3. Left hemispheric alpha and beta oscillatory dynamics progressed anteriorly during encoding and maintenance time windows.

Beamformer images (pseudo-t) averaged across high-distraction and low-distraction conditions and all participants are displayed per time bin spanning the encoding (100–1500 ms; green labels), early maintenance (1500–1850 ms; white labels), and maintenance (2100–3900 ms; purple labels) phases. Top: There was a sustained decrease in alpha (8–14 Hz) power relative to baseline in the left posterior occipital cortices during the early encoding phase, which spread anterior towards the left parietal, temporal, and frontal cortices during the second half of encoding and early maintenance period. Bottom: There was also a sustained decrease in beta (β_{full}: 14–23 Hz) power in the left occipital and inferior parietal cortices during early encoding and this extended towards more anterior and superior parietal, temporal, and frontal cortices during the second half of encoding and maintenance period with a brief increase in beta relative to baseline in the occipital cortex from 2100–2550 ms.

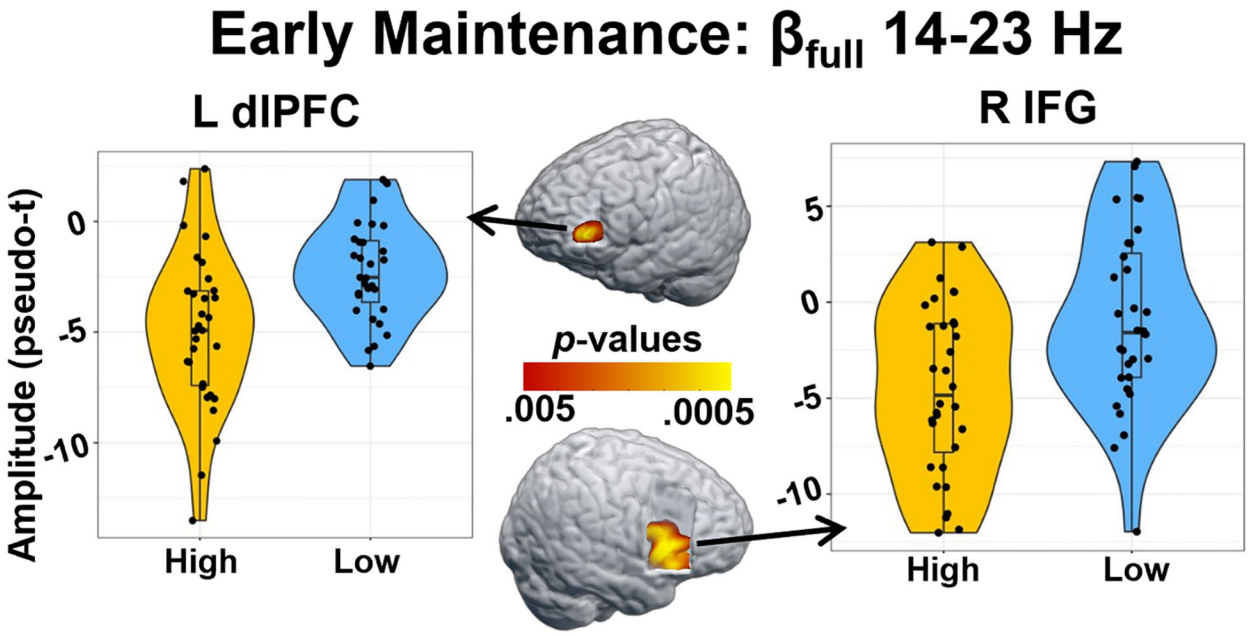

Fig. 4. Conditional differences in beta activity during the early maintenance period.

Whole-brain paired *t*-tests revealed significant differences in beta power during the early maintenance (1500–1850 ms) window, such that there were stronger beta oscillations (i.e., greater decreases in power relative to baseline) in the high-relative to the low-distraction condition in the left dorsolateral prefrontal cortex (dlPFC; $p < .005$, corrected) and right inferior frontal gyrus (IFG; $p < .005$, corrected). Violin plots show the distribution of the amplitude at the peak voxel of the significant cluster on the y-axis, with condition plotted on the x-axis. Within each violin, box plots show the median value of the amplitude with vertical lines representing values below the 25th percentile or above the 75th percentile.

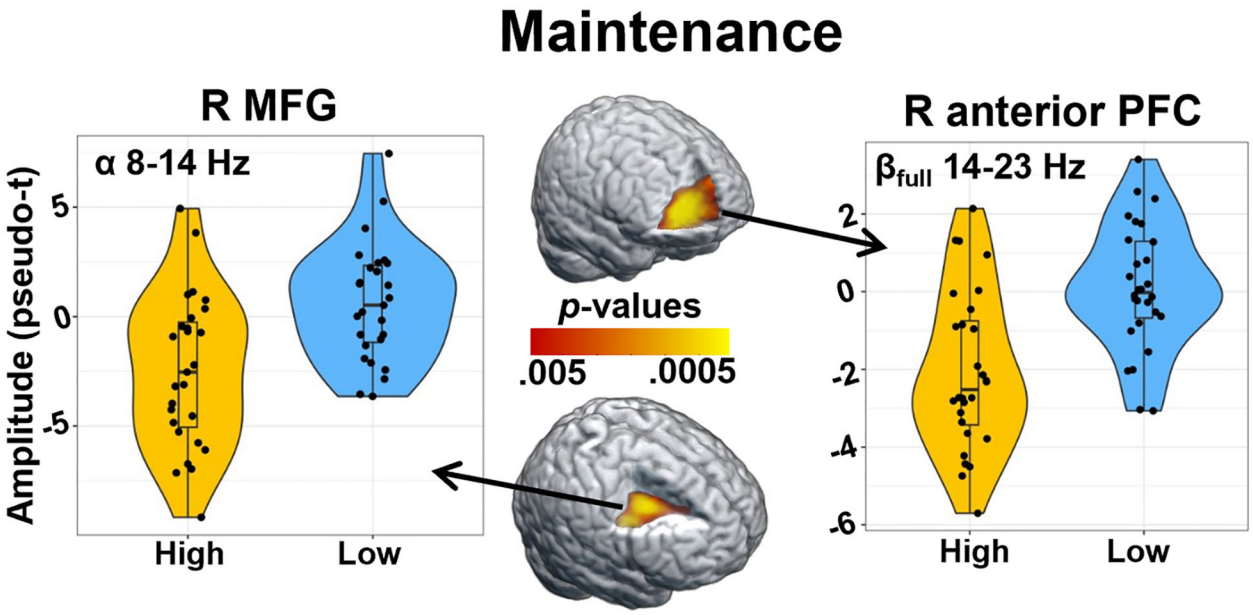

Fig. 5. Conditional differences in sustained alpha and beta activity during maintenance.

Whole-brain paired *t*-tests revealed significant differences in alpha and beta power during maintenance (2100–3900 ms), such that there were stronger oscillations (i.e., greater decreases in power relative to baseline) in the high-distraction relative to the low-distraction condition. Left: Differences in alpha (8–14 Hz) activity were found in the right middle frontal gyrus (MFG; $p < .005$, corrected). Right: Differences in beta (βfull: 14–23 Hz) activity were found in the right anterior prefrontal cortex (PFC; $p < .005$, corrected). Violin plots show the distribution of the amplitude at the peak voxel of the significant cluster on the y-axis, with condition plotted on the x-axis. Within each violin, box plots show the median value of the amplitude with vertical lines representing values below the 25th percentile or above the 75th percentile.